JCTC Journal of Chemical Theory and Computation

CHARMM Force Field Parameters for Nitroalkanes and Nitroarenes

Jeffery B. Klauda* and Bernard R. Brooks

Laboratory of Computation Biology, National Heart, Lung, and Blood Institute, National Institutes of Health, Bethesda, Maryland 20892

Received August 1, 2007

Abstract: New CHARMM force field (FF) parameters are developed for nitro compounds, referred to here as C27rn, for subsequent use in molecular dynamics (MD) simulations. The nonbonded terms are adjusted to best fit densities and hydration energies of nitropropane and nitrobenzene. High-level quantum mechanical calculations are used to obtain accurate conformational energies of nitroalkanes and nitrobenzene and to adjust the torsional potential of the CHARMM FF. For nitroalkanes, the calculated gauche (*g*) conformer of the C−C−C−N torsion is more stable than trans (*t*). Consequently, nitropropane MD simulations with C27rn result in 74% population of this *g* conformer. The C27rn FF is in excellent agreement with experiment for various bulk (density, isothermal compressibility, and heat of vaporization) and interfacial (surface tension) properties of nitropropane, nitrobutane, and nitrobenzene. MD simulations with the OPLS-AA FF for nitropropane and nitrobenzene result in similar property predictions as C27rn, except a reduced stability of the C−C−C−N *g* conformer.

1. Introduction

Compounds containing one or more nitro groups are commonly used as explosives,[1] organic solvents,[2,3] herbicides,[4] pesticides,[4] and drugs.[5,6] A few specific examples of these nitro compounds are described briefly as motivation for their general importance. In 1947, the first broad spectrum antibiotic (chloramphenicol) was discovered.[6] This early antibiotic contains a nitro group attached to a benzene ring but is not used extensively because of bacterial resistance and certain undesirable side effects. As another example, pure nitrobenzene or 2-nitrophenyl *n*-octyl ether are widely used as organic solvents.[2,3] These compounds are prominent in studies of ion transfer across interfaces with two immiscible liquids. The fluorescence of nitrobenzene with tryptophan has been important in binding studies of substrates in proteins. Specifically, sugar binding studies of the transmembrane protein lactose permease have used intrinsic Trp fluorescence with a nitro containing sugar, 6′-(*N*-dansyl)-aminohexyl-1-thio-β-D-galactopyranoside (α-NPG), to determine and quantify sugar binding.[7,8]

Although nitro compounds are of general and biological significance, only a limited number of studies have focused on developing force field (FF) parameters for use in molecular simulations.[9−13] Price et al.[13] developed nitro parameters for the OPLS-AA FF that resulted in good agreement with experimental gas-phase and liquid properties, e.g., density, heats of vaporization, and free energies of salvation, from molecular simulations. The primary focus of FF development has been nitrobenzene because of its importance as an organic solvent. An excellent comparison of nitrobenzene FFs (OPLS-AA,[13] Michael and Benjamin,[11] and Janssen et al.[9]) and experiment is discussed by Jorge et al.[10] The FF by Michael and Benjamin[11] focused on the nitrobenzene/water interface, while other FFs were only compared with bulk properties. It was found that OPLS-AA compares most favorably with experiment[10] and will be used as a benchmark in our studies.

For the CHARMM FF, a parameter set is not currently available for nitro compounds.[14] Therefore, the main purpose of this work is to develop nitro parameters consistent with CHARMM optimization procedures.[14−16] This new parameter

* Corresponding author e-mail: jbklauda@umd.edu. Current address: Department of Chemical and Biomolecular Engineering, University of Maryland, College Park, MD 20742.

10.1021/ct700191v
Published on Web 12/06/2007

set is then tested on pure liquid and interfacial systems of nitroalkanes and nitrobenzene.

Special focus in the force field development is on potential energy scans of two nitro torsional angles, i.e., C−C−N−O and C−C−C−N. Several conformational energies of nitroalkanes with the OPLS-AA FF were compared with ab initio energies at the HF/6-31g(d) level.[13] For nitroaromatics, Staikova and Cszmadia[17] used the same quantum mechanical (QM) methods to study the conformational energies about the C−C−N−O torsion. However, we have demonstrated with alkanes the importance of including electron correlation, i.e., more accurate QM methods, for torsional energies.[18,19] Consequently, highly accurate ab initio methods will be used in this study to describe the conformational energies of nitroalkanes and nitrobenzene. The FF will be adjusted accordingly to best match these QM calculations, and the methods and results will be described in the following sections.

2. Methodology

The methodologies used for fitting the CHARMM FF (2.1), ab initio calculations (2.2), and molecular dynamics simulations (2.3) for nitro compounds are described in this section.

2.1. Force Field Fitting. The potential energy $V(\hat{\mathrm{R}})$ in the CHARMM FF[14] as well as other additive FF[13,20−22] is a function of the positions of all of the atoms in the system and has the following general form:

$$V(\hat{\mathrm{R}}) = \sum_{\text{bonds}} K_b(b - b_0)^2 + \sum_{\text{angles}} K_\theta(\theta - \theta_0)^2 + \sum_{\text{dihedrals}} \left[\sum_j K_{\varphi,j}(1 + \cos(n_j\varphi - \delta_j))\right] + \sum_{\text{nonbonded pairs}} \epsilon_{ij}\left[\left(\frac{R_{\min,ij}}{r_{ij}}\right)^{12} - \left(\frac{R_{\min,ij}}{r_{ij}}\right)^{6}\right] + \sum_{\text{nonbonded pairs}} \frac{q_i q_j}{\epsilon_{\mathrm{D}} r_{ij}} \quad (1)$$

Urey-Bradley and improper dihedral terms are available in CHARMM but are not used for the nitro compounds. The parameters in the initial two intramolecular terms of eq 1 (K_b, b_0, K_θ, and θ_0) are obtained from previous fits for the OPLS-AA FF.[13] Identical methods are used in developing these force field parameters for CHARMM.[14,23] The dihedral potential is optimized based on highly accurate torsional energy scans from QM calculations on model compounds.[18,24,25] van der Waals interactions are treated by the well-known Lennard-Jones (LJ) "6-12" potential, where ϵ_{ij} is the potential energy minimum between two particles, and $R_{\min,ij}$ is the position of this minimum. The conversion factor between $R_{\min,ij}$ and σ_{ij} in other LJ potential forms is $R_{\min,ij} = 2^{1/6}\sigma_{ij}$. Last, q_i and q_j are the atomic partial charges, and ϵ_{D} is the dielectric constant.

The optimization procedure for the parameters in eq 1 is consistent with the procedure used for developing the CHARMM FF.[14−16] Parameters for only nitrogen, oxygen, and adjacent group atoms (carbons bonded to nitrogen) were adjusted to maintain the transferability of other atoms in the molecule. First, the atomic charges on the nitro compound are adjusted to best represent scaled QM calculations (details in section 2.2) of water/nitro compound interaction energies based on the TIP3P[26,27] water model. This is known as the supramolecule approach,[14] and the initial guess for the atomic charges is based on similar groups in the CHARMM FF. The LJ parameters are modified to best represent the experimental density and optimized separately for nitroalkanes and nitrobenzene to represent changes in the nitro dispersion energies due to the neighboring aromatic ring. Only the experimental density at 298.15 K for nitropropane and nitrobenzene is used for the LJ fits. Therefore, other properties, compounds, and temperatures are predictions. The dihedral parameters ($K_{\phi,j}$, n_j, and δ_j) are fitted to accurate QM conformational energies (details in section 2.2) and consist of 1−4 sets, j, per dihedral type and summed over all the dihedral angles in the molecule.

The optimization of the C27rn FF parameters is typically an iterative process and requires several changes to obtain proper convergence of the desired properties. The supermolecule approach defines the charges, but the LJ and dihedral parameters are interdependent. Changes to the LJ terms are made until the bulk density is in satisfactory agreement with experiment. Consequently, the dihedral parameters are optimized for each LJ parameter set.

2.2. Quantum Mechanical Calculations. The Gaussian03 suite of programs[28] was used for the following QM calculations: (1) conformational states of nitropropane, nitrobutane, nitropentane, and nitrobenzene and (2) water interacting with individual nitro compounds. The conformational minima were optimized using tight convergence criteria (1.5×10^{-4} and 1.0×10^{-4} hartree/bohr for maximum and rms force) and a starting structure near the corresponding conformation, i.e., trans or gauche. In addition to the minima, conformations between the local minima and barriers are optimized. This was done using the Berny Algorithm[29] by fixing a corresponding dihedral angle on a transition state (TS) pathway. Geometry optimizations for single molecule conformations were performed at MP2/cc-pVDZ, while HF/6-31g(d) was used for water/nitro interactions. This lower level of theory for the dimer was used to be consistent with the CHARMM parametrization of the Coulombic terms.[14]

The HM-IE method[30] was used to estimate the energy of each individual molecular conformation of nitro compounds at the CCSD(T) level with a basis set larger than that used to obtain the optimized geometry. This method estimates molecular properties by assuming that the separate effects of electron correlation and basis set size are additive. These hybrid or compound QM methods, such as the Gaussian-3,[31,32] Dunning and Peterson,[33] and HM-IE,[30] estimate energies of CCSD(T) with a large basis set (LBS) by calculating CCSD(T) with a smaller basis set (SBS) and adding a correction based on the difference between MP2 energies with a LBS and a SBS as follows

$$E^{\text{conf}}[\text{CCSD(T)/LBS}] = E^{\text{conf}}[\text{CCSD(T)/SBS}] + (E^{\text{conf}}[\text{CCSD(T)/LBS}] - E^{\text{conf}}[\text{CCSD(T)/SBS}])$$

$$\cong E^{\text{conf}}[\text{CCSD(T)/SBS}] + (E^{\text{conf}}[\text{MP2/LBS}] - E^{\text{conf}}[\text{MP2/SBS}])$$

$$\equiv E^{\text{conf}}[\text{MP2:CC}] \quad (2)$$

where E^{conf} is the energy of the conformer, and the difference between CCSD(T)/LBS and CCSD(T)/SBS is approximated at the MP2 level. A SBS of cc-pVDZ and LBS of cc-pVQZ was used here and also found previously to be an accurate measure of CCSD(T)/cc-pVQZ for linear alkanes.[18]

As an additional accuracy measure of the dihedral potential, the curvatures for selected trans or gauche wells were estimated by taking the second derivative of the energy, $V(\phi)$, with respect to the angle by means of fitting a parabolic function

$$V(\phi) = k(\phi - \phi_0)^2 + l(\phi - \phi_0) + m \quad (3)$$

where k, l, and m are fit to either the QM energy or empirical force field predictions with energies up to 2 kcal/mol higher than the local minima.

2.3. Molecular Dynamics Simulations. Simulations were performed with CHARMM[34] using C27r for the alkane portion of the FF[18,19] and adjustments to the nitro force field, referred to here as C27rn. Nitrobenzene and nitropropane simulations with OPLS-AA are also performed for comparison with C27rn. The leapfrog Verlet algorithm was used with cubic periodic boundary conditions. A time step of 1 fs was applied to ensure time step artifacts did not affect our calculated properties. LJ interactions were smoothed by a switching function over 8−10 Å. Isobaric−isothermal ensemble (NPT) simulations were run with long-range electrostatics and LJ corrections. The particle mesh Ewald (PME)[35] method was used for the long-range electrostatic contribution (beyond 10 Å) to the total energy with $\kappa = 0.34$ Å^{-1} and a fast-Fourier grid density of about 1 Å^{-1}. The isotropic periodic sum (IPS) method[36] was used to obtain the long-range correction in LJ at an effective infinite cutoff. This PME/IPS method has been found to be accurate in bulk and interfacial systems.[37] All hydrogen atoms were constrained using the SHAKE algorithm.[38] The extended system formalism was used to maintain the temperature via the Hoover thermostat[39] and/or pressure[40,41] with a thermostat coupling constant of 20 000 kcal mol^{-1} ps^{-2} and a piston mass of 2000 amu.

Initial conformations for bulk nitropropane, nitrobutane, and nitrobenzene were obtained by placing 320, 256, and 200 molecules, respectively, on an even grid in random orientations. With these starting conformations, the energy was minimized with the steepest descent routine for 200 steps to reduce unfavorable van der Waals contacts. The velocities were then set to the desired temperature, and an equilibration period of 500 ps was used for all simulations to ensure full equilibration. The coordinates were saved every 1 ps for a total simulation time of 2 ns for simulations at 288.15, 293.15, and 303.15 K, but a simulation time of 5 ns was used for the 298.15 K runs. For vapor simulations, N simulations with a single molecule were run for 500 ps after 50 ps of equilibration. Coordinates from the end of each liquid simulation at 298.15 K were used as N initial coordinates for the vapor simulations.

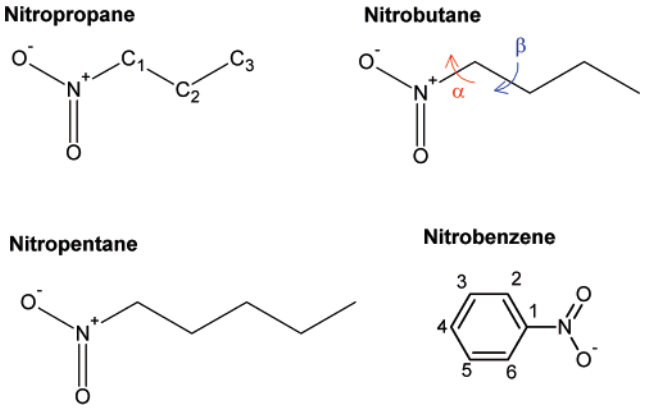

Figure 1. Model compounds used in QM calculations to develop the C27rn FF. The atom types for the aliphatic carbons are labeled on nitropropane, and the dihedrals are labeled on nitrobutane.

Table 1. Nonbonded Parameters for C27rn[a]

atom	description/location	q [e]	ϵ [kcal/mol]	$R_{\min}/2$ [Å]
N	nitroalkane	+0.50	−0.160	1.837
O	nitroalkane	−0.40	−0.120	1.700
C	C_1 in nitroalkane	+0.16	−0.056	2.010
H	attached to C_1	+0.07	−0.028	1.340
N	nitroarene	+0.50	−0.120	1.850
O	nitroarene	−0.40	−0.100	1.770
C	C_6 in nitrobenzene	+0.34	−0.070	1.992
C	C_1 or C_5 in nitrobenzene	−0.18	−0.070	1.992
H	attached to C_1 or C_5	+0.16	−0.046	1.100

[a] See Figure 1 for labeling nomenclature.

Table 2. Torsional Parameters for C27rn[a]

	K_ϕ [kcal/mol]	n	δ [deg]
CH2−CH2−N−O	0.060	2	0
CH3(2)−CH2−CH2−N	0.084	4	0
	0.360	3	0
	0.151	2	0
	0.133	1	180
HA−CA−CA−N	1.000	2	180
CA−CA−CA−N	6.140	2	180
CA−CA−N−O	1.100	2	180

[a] CH3 and CH2 are for nitroalkanes and CA is for nitrobenzene.

Densities, heat of vaporization, isothermal compressibilities, and self-diffusivities were calculated. Standard errors were estimated from block averages.[42] Isothermal compressibilities were calculated from

$$\beta_T = -\frac{1}{V}\left(\frac{\partial V}{\partial P}\right)_T = \frac{\langle \delta V^2 \rangle}{V k_b T} \quad (4)$$

where V is the volume, $\langle \delta V^2 \rangle$ is the volume fluctuation, and k_b is Boltzmann's constant. The 5-ns simulations at 298.15 K were used to calculate eq 4. The slope of the mean squared displacement versus time was used to determine the apparent self-diffusivity for the periodic boundary condition, D_{PBC}, using a weighted least squared fit with weights obtained from averages of 8−10 subgroups of molecules per trajectory. The self-diffusivity was corrected for system-size effects using the hydrodynamic model of Yeh

Table 3. Molecular Structures of Nitro Compounds from MP2/cc-pVDZ (except Nitropropane Also with cc-pVTZ) with Atom Numbering and Dihedral Angles as Shown in Figure 1[a]

	nitropropane				nitrobutane		nitropentane		nitrobenzene	
	t-DZ	*g*-DZ	*t*-TZ	*g*-TZ	*t*	*g*	*t*	*g*	MP2	exp[b]
C_1-N	1.50	1.50	1.49	1.49	1.50	1.50	1.50	1.50	1.48	1.49
C_1-C_2	1.52	1.53	1.52	1.52	1.52	1.53	1.52	1.53	1.40	1.40
N═O	1.23	1.23	1.23	1.23	1.23	1.23	1.23	1.23	1.23	1.22
$\angle C_1-N═O$	117.1	117.0	117.1	117.2	117.1	117.0	117.1	117.0	117.3	117.3
$\angle O═N═O$	125.9	125.9	125.6	125.5	125.9	125.9	125.9	125.9	125.4	125.3
$\angle C_1-C_2-N$	110.6	109.1	109.2	109.4	110.5	109.0	110.6	109.0	118.7	118.3
α	121.7	111.1	88.6	115.1	121.6	110.2	121.9	110.1	0.0	
	−57.9	−66.7	−88.6	−63.3	−58.0	−67.5	−57.7	−67.6		
β	179.7	−60.7	180.0	−59.0	180.0	−61.1	179.6	−60.9	0.0	

[a] Distances are in Å and angles are in degrees. For the nitroalkanes, structures are listed in the (CCCN) trans (*t*) and gauche (*g*) conformation. [b] The experimental electron diffraction data for nitrobenzene.[44,45]

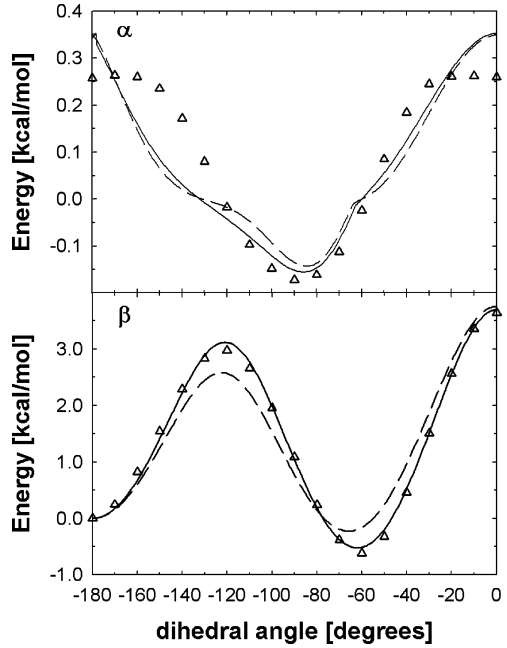

Figure 2. Conformational energies of nitropentane as a function of α (C_2-C_1-N-O) and β ($C_3-C_2-C_1-N$) torsional angles. The corresponding dihedral is fixed for each point on the panel, but all other degrees of freedom are minimized. The symbols are QM energies (MP2:CC), the solid line is C27rn, and the dashed line is OPLS-AA.

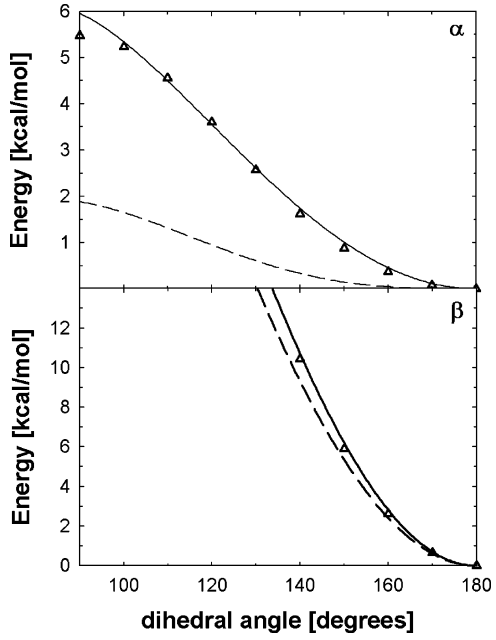

Figure 3. Conformational energies of nitrobenzene as a function of α and β torsional angles. The corresponding dihedral is fixed for each point on the panel, but all other degrees of freedom are minimized. The symbols are QM energies (MP2:CC), the solid line is C27rn, and the dashed line is OPLS-AA.

and Hummer[43] of a particle surrounded by a solvent with a viscosity, η

$$D_s = D_{PBC} + \frac{k_B T \xi}{6\pi\eta L} \tag{5}$$

where L is the cubic box length and $\xi = 2.837297$.[43]

The heat of vaporization was calculated from

$$\Delta H^{vap} = \langle U_{ig} \rangle - \frac{\langle U_l \rangle}{N} + RT \tag{6}$$

where $\langle U_l \rangle$ is the average internal energy over time (sum of intra- and intermolecular energies) of the liquid state, N is the total number of molecules, and $\langle U_{ig} \rangle$ is the average ideal gas internal energy. The average liquid internal energy was obtained from the liquid simulations and N gas simulations to obtain $\langle U_{ig} \rangle$.

The surface tension was evaluated from

$$\gamma = 0.5\langle L_z[P_{zz} - 0.5(P_{xx} + P_{yy})] \rangle \tag{7}$$

where L_z is the size of the simulation box normal to the interface, P_{zz} is the normal component of the internal pressure tensor, and P_{xx} and P_{yy} are the tangential components. The MD simulations here contain two interfaces (a liquid film with vapor at the top and bottom, see ref 37), so a prefactor of 0.5 is required to obtain γ on a per interface basis.

3. Results and Discussion

The parametrization of the LJ, electrostatics, and dihedral terms is iterative, but the results discussed here are based on the optimal values in Tables 1 and 2. The ab initio calculations on the molecular structure and torsional profiles are presented first. Then, the conformational energies of the

Table 4. Nitroalkane Conformer Energies in kcal/mol Relative to the All-Trans State of the β Torsion[a]

		ΔE_g	$\Delta E^{\dagger}_{t/g}$	$\Delta E^{\dagger}_{g/g}$
C_3NO_2	MP2:CC	−0.60	3.14	3.68
	C27rn	−0.49	3.13	3.64
	OPLS-AA	0.06	2.64	4.04
		ΔE_g	$\Delta E^{\dagger}_{t/g}$	$\Delta E^{\dagger}_{g/g}$
C_4NO_2	MP2:CC	−0.61	2.96	3.65
	C27rn	−0.56	3.10	3.65
	OPLS-AA	−0.24	2.57	3.73
		ΔE_g	$\Delta E^{\dagger}_{t/g}$	$\Delta E^{\dagger}_{g/g}$
C_5NO_2	MP2:CC	−0.62	2.98	3.64
	C27rn	−0.52	3.12	3.70
	OPLS-AA	−0.23	2.58	3.76

[a] MP2:CC is the approximate CCSD(T)/cc-pVQZ energy using eq 2. C27rn is the modified C27r force field. The energy of the transition state between local minima *i* and *j* relative to the all-trans state is denoted as $\Delta E^{\dagger}_{ij}$.

new force field (C27rn) are compared with the QM calculations as well as the OPLS-AA.[13] Finally, C27rn is tested with bulk and interfacial simulations and compared with experiment and OPLS-AA.

3.1. Molecular Structures and Torsional Profiles. *3.1.1. Ab Initio Calculations.* The geometry of the nitro compounds (Figure 1) is optimized using MP2, and the distances, angles, and torsional angles are listed in Table 3. The agreement between electron diffraction[44,45] and MP2/cc-pVDZ for nitrobenzene is excellent, i.e., deviations of ≤0.01 Å and 0.4°. For nitroalkanes, there are two minima of the C−C−C−N torsion (β), i.e., *t*-trans and *g*-gauche (g^- is shown here but equivalent to g^+). Double- and triple-ζ basis set optimizations for the *t* conformation of nitropropane result in a noticeable difference for the C−C−N−O torsion angle, α (Table 3). However, in terms of conformational energy (of most interest to this work) HM-IE corrects for this basis set effect. Moreover, there are negligible differences with other structural properties of the *t* conformer and all properties of the *g* conformer. Therefore, MP2/cc-pVDZ optimizations will be used for their efficiency and reasonable accuracy with larger nitroalkanes. Previous calculations with B3LYP/6-31g(d)[46] result in *t* structures similar to those in Table 3 but may result in similar basis set problems. There are other structural differences between the *t* and *g* conformation, i.e., $\angle C_1-C_2-N$ and α are reduced in the *g* conformation compared to *t*. However, other internal geometry values are not influenced by this change in the β torsion.

Quantum mechanical conformational energies of the α and β torsions of the four nitro compounds were calculated using eq 2 with a total of 129 conformations. The torsional profiles for nitropentane and nitrobenzene are shown as examples in Figures 2 and 3, respectively. The β torsion is alkane-like with two minima (*t* and *g*). For alkanes, high-level ab initio QM calculations on pentane through heptane yield a ΔE_g (energy difference from the all-trans state) slightly higher than +0.5 kcal/mol.[18,47−49] However, the *g* conformation in nitroalkanes is lower in energy, i.e., $\Delta E_g = -0.6$ kcal/mol (see Table 4). The terminal nitrogen and oxygen on this β torsion stabilize the *g* state. Similarly, for nitroalkanes there is a greater than 1 kcal/mol decrease in the cis conformational energy compared to alkanes. Although there are differences in *g* and cis energies, the conformational energy of the transition from the *t* to *g* state $\Delta E^{\dagger}_{t/g}$ is similar to that of an alkane (3 kcal/mol).[18]

The conformational energy barriers for nitroalkanes are lower than nitrobenzene. The conformational space is restricted because the nitro group is attached to an aromatic ring (Figure 3). Therefore, the lowest energy conformation of nitrobenzene is when the nitrogen and oxygen atoms are in the same plane as the carbons, i.e., a planar molecule.

3.1.2. Empirical Potentials. A root-mean squared error objective function was used to fit the set of nitro dihedrals to the high-level QM energies discussed above. Table 2 lists five sets of dihedrals fit to the ab initio calculations, denoted here as C27rn. Only the C−C−C−N dihedral required more than one term. This is similar to the alkane C−C−C−C torsion in the C27r FF,[18] where multiple torsional terms were needed to accurately fit conformational energies.

The molecular structure of the nitroalkanes and nitrobenzene with C27rn is listed in Table 5. The bond lengths are nearly identical between the MP2/cc-pVDZ and C27rn optimized structures. $\angle C_1-C_2-N$ is slightly larger with C27rn but only deviates by 3−4°. The optimized *t* conformation with C27rn results in an α torsion in good agreement with the correct value using MP2/cc-pVTZ. There is also excellent agreement for the value of the β torsion of the *g* conformation with less than 1° difference between QM and C27rn.

The calculated nitroalkane minima and transition state (TS) energies with C27rn and OPLS-AA are compared with MP2:CC in Table 4. The absolute average deviation (AAD) from MP2:CC for these conformations with C27rn and OPLS-AA is 0.07 and 0.36 kcal/mol, respectively. The AAD for just ΔE_g is larger with OPLS-AA (0.47 kcal/mol) and similar for C27rn (0.09 kcal/mol). Overall, C27rn is superior to OPLS-AA in these conformational energies. OPLS-AA is parametrized on smaller molecule conformations of nitroalkanes with HF/6-31g(d). Since low-level QM calculations are known to result in inaccurate dispersion energies,[50,51] the large discrepancy in ΔE_g is not surprising for OPLS-AA.

The correct curvature of *t* and *g* wells is of greater importance than slight inaccuracies of minima energies, because there is an increased availability of dihedral angles at a given temperature.[18] Table 6 lists the curvature for the minima of the *t* and *g* conformers of the β torsion calculated from eq 3. The curvature of the C27rn wells compared to OPLS-AA is in better agreement with MP2:CC with an overall AAD of 0.16×10^{-3} and 0.63×10^{-3} kcal mol^{-1} deg^{-2}, respectively. The QM curvature of the *g* well is greater than *t* due to electron repulsion. For OPLS-AA the *g* well is too broad (Table 6) because of the lack of conformations other than the minima and transitional barrier and a less accurate QM method.[13]

OPLS-AA and C27rn both follow the conformational energies of MP2:CC qualitatively as shown in Figures 2 and 3, but C27rn is noticeably in better agreement with QM. Although there are differences with QM and C27rn for the

Table 5. Molecular Structures of Nitro Compounds with C27rn

	nitropropane		nitrobutane		nitropentane		nitrobenzene	
	t	*g*	*t*	*g*	*t*	*g*	C27rn	exp[a]
C_1-N	1.50	1.50	1.50	1.50	1.50	1.50	1.47	1.49
C_1-C_2	1.54	1.54	1.54	1.54	1.54	1.54	1.42	1.40
N=O	1.23	1.23	1.23	1.23	1.23	1.23	1.23	1.22
$\angle C_1-N=O$	117.5	117.4	117.5	117.5	117.5	117.5	117.5	117.3
$\angle O=N=O$	124.5	124.2	124.6	124.4	124.5	124.4	125.0	125.3
$\angle C_1-C_2-N$	113.8	113.8	113.7	113.9	113.7	113.9	121.7	118.3
α	85.8	115.2	86.4	108.7	85.9	110.1	0.0	
	−85.5	−75.4	−86.2	−78.6	−86.0	−77.8		
β	180.0	−61.4	180.0	−61.9	180.0	−61.9	0.0	

[a] The experimental electron diffraction data for nitrobenzene.[44,45] Atom numbering and dihedral angles as shown in Figure 1.

Table 6. Curvatures ($2k$ in Eq 3) of Trans And Gauche Conformations[a]

state	molecule	MP2:CC	C27rn	OPLS-AA
t	C_3NO_2	2.57	2.61	2.26
g	C_3NO_2	4.26	3.98	2.99
t	C_4NO_2	2.42	2.60	2.23
g	C_4NO_2	4.14	3.98	3.16
t	C_5NO_2	2.42	2.61	2.23
g	C_5NO_2	4.18	3.98	3.16

[a] In units of 10^{-3} kcal mol^{-1} deg^{-2}.

Table 7. C27rn Simulation Averages and Standard Errors for Dipole Moment (μ), Density (ρ), Isothermal Compressibility (β_T), Diffusivities (D_{PBC} and D_s), and Heat of Vaporization (ΔH^{vap}) at 298.15 K[a]

		C_3NO_2	C_4NO_2	NB
μ	C27rn	4.80 ± 0.00	4.80 ± 0.00	4.53 ± 0.00
[D]	OPLS-AA	3.82 ± 0.00		3.33 ± 0.00
	exp[53]	3.59		4.22
ρ	C27rn	0.999 ± 0.007	0.974 ± 0.007	1.208 ± 0.009
[g/cm^3]	OPLS-AA	0.974 ± 0.008		1.154 ± 0.009
	exp[52]	0.996	0.968	1.198
β_T	C27rn	6.27 ± 0.15	4.64 ± 0.16	4.17 ± 0.10
[10^{-10} m^2/N]	OPLS-AA	11.34 ± 0.09		4.57 ± 0.12
	exp[53]			5.23
D_{PBC}	C27rn	0.712 ± 0.070	0.595 ± 0.010	0.370 ± 0.060
[10^{-5} cm^2/s]	OPLS-AA	0.580 ± 0.083		0.706 ± 0.072
	exp[53]			1.08
D_s	C27rn	0.929 ± 0.070	0.815 ± 0.010	0.477 ± 0.060
[10^{-5} cm^2/s]	OPLS-AA	0.792 ± 0.083		0.812 ± 0.072
	exp[53]			1.08
ΔH^{vap}	C27rn	12.72 ± 0.38		14.19 ± 0.60
[kcal/mol]	OPLS-AA			13.05 ± 0.48
	exp[53]	10.37		13.15

[a] β_T and ΔH^{vap} were calculated from eqs 4 and 6, respectively. D_{PBC} is the apparent self-diffusivity obtained directly from the mean squared displacement in the simulations, and the corrected self-diffusivity, D_s, is obtained from eq 5.

Table 8. Surface Tension of Nitropropane and Nitrobenzene in dyn/cm Compared with Experiment[53]

		C_3NO_2	NB
293.15 K	C27rn	31.51 ± 0.87	43.52 ± 0.38
	exp	30.64	42.70
303.15 K	C27rn	29.49 ± 0.35	41.94 ± 0.64
	exp	29.61	42.17

α torsion in nitroalkanes (Figure 2), they are small for an essentially freely rotating potential at 298.15 K. Since the cause for this discrepancy is the LJ and electrostatic energies, a polarizable FF may improve this agreement between QM and C27rn. For the β torsion, the TS energy is lower than QM with OPLS-AA, and the *g* minimum is skewed for nitropentane (Figure 2), where as C27rn follows the QM energies almost exactly. The α adiabatic surface with OPLS-AA and C27rn is similar and in satisfactory agreement with MP2:CC for nitroalkanes. However, OPLS-AA significantly underpredicts the out-of-plane energy of the oxygen in nitrobenzene (>3 kcal/mol), where C27rn results in excellent agreement with MP2:CC.

3.2. Molecular Dynamics Simulations. The validity of the new C27rn FF for nitro compounds was tested on bulk and interfacial systems containing nitropropane, nitrobutane, and nitrobenzene. The nitrogen and oxygen LJ parameters for nitroalkanes were adjusted to best fit the density of nitropropane at 298.15 K, and the simulated density is in perfect agreement with experiment.[52] The temperature dependence of the density is shown in Figure 4, and the AAD of C27rn is only 0.29 g/cm^3. There is similar agreement for the densities of nitrobutane and nitrobenzene with an AAD of 0.53 and 0.85 g/cm^3, respectively (Figure 4). The LJ nitrogen and oxygen parameters for nitrobenzene were allowed to vary from nitroalkanes to obtain accurate densities at 298.15 K. The density of OPLS-AA for nitropropane and nitrobenzene are slightly lower than experiment (0.974 and 1.154 g/cm^3, respectively), but the LJ parameters for nitrogen and oxygen were identical for all nitro compounds in the OPLS-AA FF.

As shown previously, the conformational energies about the β torsional surface of nitroalkanes differ between OPLS-AA and C27rn. Consequently, the conformational probabilities for the β torsion are also quite different (Figure 5). There is an increased population of *g* conformations with C27rn (74% versus 57% for C27rn and OPLS-AA, respectively). This increase in *g* population is similar to MD simulations of pure alkanes[18,19] with a more accurate description of the C−C−C−C torsional surface. Contrary to nitroalkanes, experimental data are available for conformational populations of alkanes, and the C27r force field fit to QM (MP2:CC) is in excellent agreement with experiment.[18]

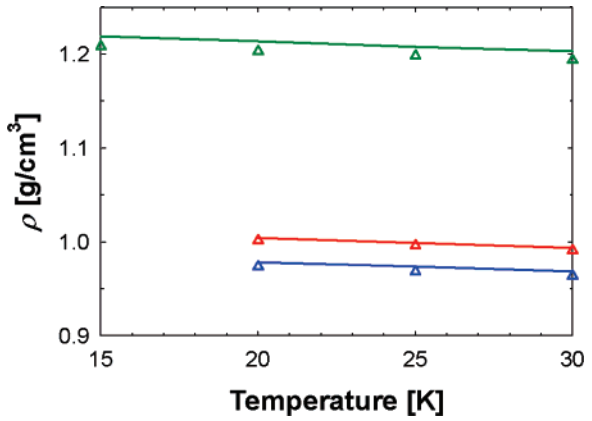

Figure 4. The density of nitrobenzene (green), nitropropane (red), and nitrobutane (blue) as a function of temperature for C27rn (lines) and experiment (triangles).

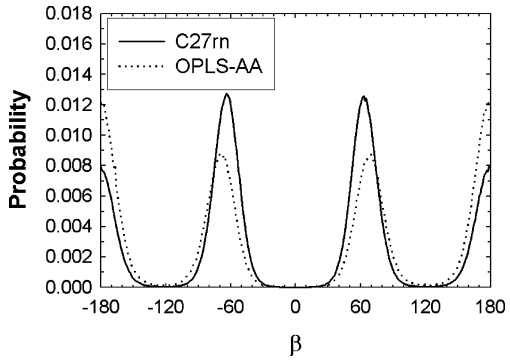

Figure 5. The probability of the β ($C_3-C_2-C_1-N$) torsional angle of nitropropane.

This implies that these results for nitro compounds using the same QM methods would be accurate if experimental data were available.

The molecular dipoles (μ) of nitropropane and nitrobenzene with C27rn are consistently higher than experiment.[53] An elevated μ is expected and typical of the CHARMM FF because the experimentally measured values are usually in the gas phase and polarization of the liquid phase results in an increase in the dipole moment. MD simulations with OPLS-AA result in an average μ of 3.82 and 3.33 D for nitropropane and nitrobenzene, respectively, which are significantly lower than experiment.

The radial distribution functions (RDFs) between oxygen and carbon calculated from the bulk simulations are shown in Figure 6 for nitrobenzene (top) and nitropropane (bottom). The RDFs for OPLS-AA and C27rn are similar in shape with some subtle differences in peak locations. For example, the O/C distance is slightly larger between molecules for OPLS-AA and consistent with an increase in the overall density of the C27rn liquids. There is a preference of oxygen to interact closely with the *para* (C4) and *meta* (C3 and C5) carbons in nitrobenzene (Figure 1, data not shown for *para*) but at a distance greater than a C−H···O hydrogen bond. However, interactions are weaker with the more negative *ortho* carbons (C2 and C6). A similar trend is seen for nitropropane with oxygen interacting more strongly with the C3 carbon. Moreover, the first peak height is reduced with OPLS-AA for the O/C1 and O/C3 RDFs.

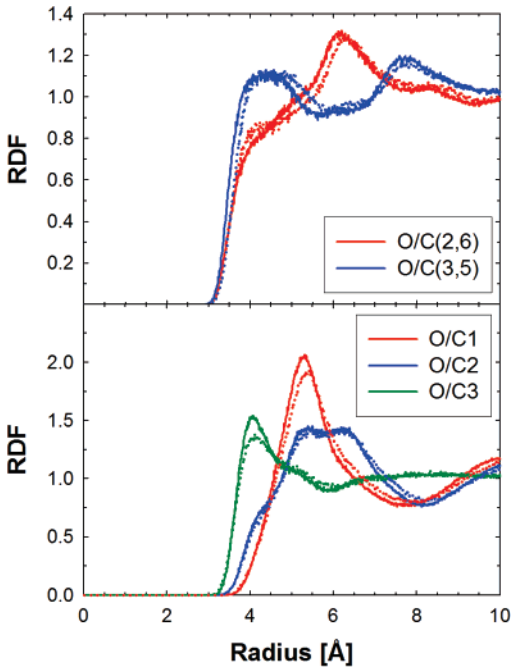

Figure 6. Radial distribution functions (RDF) between oxygen and carbon of nitrobenzene (top) and nitropropane (bottom). The C27rn results are in solid lines, and the OPLS-AA results are in dotted lines.

The enthalpy of vaporization (ΔH^{vap}) is comparable to experiment[53] for nitropropane and nitrobenzene (Table 7). C27rn results in ΔH^{vap} that is slightly larger than experiment for nitropropane but within statistical error for nitrobenzene. The OPLS-AA FF is in slightly better agreement with experiment (13.05 kcal/mol for nitrobenzene) but at the cost of a lower bulk density. The isothermal compressibilities (β_T) of C27rn and OPLS-AA are lower than experiment for nitrobenzene by 1.06 and 0.66 $\times$ 10^{-10} m^2/N, respectively.

The diffusion constant (D_s) and surface tension (γ) were used as additional measures for the accuracy of C27rn. D_s of nitrobenzene is smaller than experiment for C27rn and OPLS-AA (0.812 $\times$ 10^{-5} cm^2/s). The nitrobenzene diffusion constant is larger for OPLS-AA compared to C27rn, but the OPLS-AA D_s for nitropropane is 15% smaller than C27r. This flip-flop in D_s order may not be the result of inaccurate nitro parameters, rather differences in the parameters for the alkane or benzene portion of the respective FF. The agreement with experiment is improved for γ (Table 8) compared to D_s with an AAD of 1.6 and 1.2 dyn/cm for nitropropane and nitrobenzene, respectively.

4. Summary

Force field parameters for the important nitro group have been optimized for use with the CHARMM FF. The conformational energies of nitroalkanes and nitrobenzene were best fit to accurate and high-level QM calculations. Consequently, MD simulations with C27rn result in an increased population of *g* conformers compared to OPLS-AA. Bulk and interfacial properties from the nitro simulations with C27rn are in excellent agreement with experiment, especially densities, heats of vaporization, and surface tensions. However, the calculated diffusion constant of liquid

nitrobenzene with both OPLS-AA and C27rn is lower than experiment. Simple nonpolarizable FF models can accurately model most liquid properties but without more complex functions, such as polarizability, not all parameters will be in excellent agreement with experiment. Since these new parameters accurately represent interaction energies between water and nitro compounds and pure component properties, C27rn can be used in simulations of biologically relevant compounds, such as antibiotics with nitro groups or sugar analogs as substrates in membrane proteins.

Acknowledgment. This research was supported in part by the Intramural Research Program of the NIH, National Heart, Lung and Blood Institute. Some of the simulation results utilized the high-performance computational capabilities of the Biowulf PC/Linux cluster at the National Institutes of Health, Bethesda, MD (http://biowulf.nih.gov). We would also like to thank Prof. Alexander MacKerell, Jr., for providing us with initial LJ and charge parameters for the nitro containing compounds.

References

(1) Spain, J. C. Biodegradation of Nitroaromatic Compounds. *Annu. Rev. Microbiol.* **1995**, *49*, 523.

(2) Marcus, Y. *Ion Properties*; Marcel-Dekker: New York, 1997.

(3) Scholz, F.; Schroder, U.; Gulaboski, R. *Electrochemistry of Immobilized Particles and Droplets*; Springer: Heidelberg, Berlin, 2005.

(4) Harrison, M. A. J.; Barra, S.; Borghesi, D.; Vione, D.; Arsene, C.; Olariu, R. L. Nitrated phenols in the atmosphere: a review. *Atmos. Environ.* **2005**, *39*, 231.

(5) Ahlner, J.; Andersson, R. G. G.; Torfgard, K.; Axelsson, K. L. Organic Nitrate Esters-Clinical Use And Mechanisms Of Actions. *Pharmacol. Rev.* **1991**, *43*, 351.

(6) Balbi, H. J. Chloramphenicol: A review. *Pediatr. Rev.* **2004**, *25*, 284.

(7) Nie, Y. L.; Smirnova, I.; Kasho, V.; Kaback, H. R. Energetics of ligand-induced conformational flexibility in the lactose permease of Escherichia coli. *J. Biol. Chem.* **2006**, *281*, 35779.

(8) Smirnova, I. N.; Kasho, V. N.; Kaback, H. R. Direct sugar binding to LacY measured by resonance energy transfer. *Biochemistry* **2006**, *45*, 15279.

(9) Janssen, R. H. C.; Theodorou, D. N.; Raptis, S.; Papadopoulos, M. G. Molecular simulation of static hyper-Rayleigh scattering: A calculation of the depolarization ratio and the local fields for liquid nitrobenzene. *J. Chem. Phys.* **1999**, *111*, 9711.

(10) Jorge, M.; Gulaboski, R.; Pereira, C. M.; Cordeiro, M. Molecular dynamics study of nitrobenzene and 2-nitrophenyloctyl ether saturated with water. *Mol. Phys.* **2006**, *104*, 3627.

(11) Michael, D.; Benjamin, I. Molecular dynamics simulation of the water|nitrobenzene interface. *J. Electroanal. Chem.* **1998**, *450*, 335.

(12) Price, D. J.; Brooks, C. L. Detailed considerations for a balanced and broadly applicable force field: A study of substituted benzenes modeled with OPLS-AA. *J. Comput. Chem.* **2005**, *26*, 1529.

(13) Price, M. L. P.; Ostrovsky, D.; Jorgensen, W. L. Gas-phase and liquid-state properties of esters, nitriles, and nitro compounds with the OPLS-AA force field. *J. Comput. Chem.* **2001**, *22*, 1340.

(14) MacKerell, A. D., Jr. Empirical force fields for biological macromolecules: Overview and issues. *J. Comput. Chem.* **2004**, *25*, 1584.

(15) MacKerell, A. D., Jr. Interatomic Potentials: Molecules. In *Handbooks of Material Modeling*; Yip, S., Ed.; Springer: The Netherlands, 2005; p 509.

(16) MacKerell, A. D., Jr. Atomistic Models and Force Fields. In *Computational Biochemistry and Biophysics*; Becker, O. M., MacKerell, A. D., Jr., Roux, B., Watanabe, M., Eds.; Marcel Dekker: New York, 2001; p 7.

(17) Staikova, M.; Csizmadia, I. G. Ab initio investigation of internal rotation in conjugated molecules and the orientation of NO2 in nitroaromatics: nitrobenzene, o-monofluoro- and o,o′-difluoro-nitrobenzenes. *J. Mol. Struct.* (THEOCHEM) **1999**, *467*, 181.

(18) Klauda, J. B.; Brooks, B. R.; MacKerell, A. D., Jr.; Venable, R. M.; Pastor, R. W. An Ab Initio Study on the Torsional Surface of Alkanes and its Effect on Molecular Simulations of Alkanes and a DPPC Bilayer. *J. Phys. Chem. B* **2005**, *109*, 5300.

(19) Klauda, J. B.; Pastor, R. W.; Brooks, B. R. Adjacent gauche stabilization in linear alkanes: Implications for polymer models and conformational analysis. *J. Phys. Chem. B* **2005**, *109*, 15684.

(20) Cornell, W. D.; Cieplak, P.; Bayly, C. I.; Gould, I. R.; Merz, K. M.; Ferguson, D. M.; Spellmeyer, D. C.; Fox, T.; Caldwell, J. W.; Kollman, P. A. A 2nd Generation Force-Field for the Simulation of Proteins, Nucleic-Acids, and Organic-Molecules. *J. Am. Chem. Soc.* **1995**, *117*, 5179.

(21) Jorgensen, W. L.; Maxwell, D. S.; Tiradorives, J. Development and testing of the OPLS all-atom force field on conformational energetics and properties of organic liquids. *J. Am. Chem. Soc.* **1996**, *118*, 11225.

(22) Schuler, L. D.; Daura, X.; Van Gunsteren, W. F. An improved GROMOS96 force field for aliphatic hydrocarbons in the condensed phase. *J. Comput. Chem.* **2001**, *22*, 1205.

(23) MacKerell, A. D., Jr.; Bashford, D.; Bellott, M.; Dunbrack, R. L.; Evanseck, J. D.; Field, M. J.; Fischer, S.; Gao, J.; Guo, H.; Ha, S.; Joseph-McCarthy, D.; Kuchnir, L.; Kuczera, K.; Lau, F. T. K.; Mattos, C.; Michnick, S.; Ngo, T.; Nguyen, D. T.; Prodhom, B.; Reiher, W. E.; Roux, B.; Schlenkrich, M.; Smith, J. C.; Stote, R.; Straub, J.; Watanabe, M.; Wiorkiewicz-Kuczera, J.; Yin, D.; Karplus, M. All-atom empirical potential for molecular modeling and dynamics studies of proteins. *J. Phys. Chem. B* **1998**, *102*, 3586.

(24) Feig, M.; MacKerell, A. D., Jr.; Brooks, C. L. Force field influence on the observation of π-helical protein structures in molecular dynamics simulations. *J. Phys. Chem. B* **2003**, *107*, 2831.

(25) Woodcock, H.; Moran, D.; Pastor, R. W.; MacKerell, A. D., Jr.; Brooks, B. R. Ab initio modeling of glycosyl torsions and anomeric effects in a model carbohydrate: 2-Ethoxy Tetrahydrophyran. *Biophys. J.* **2007**, *93*, 1.

(26) Durell, S. R.; Brooks, B. R.; Bennaim, A. Solvent-Induced Forces between Two Hydrophilic Groups. *J. Phys. Chem.* **1994**, *98*, 2198.

(27) Jorgensen, W. L.; Chandrasekhar, J.; Madura, J. D.; Impey, R. W.; Klein, M. L. Comparison of Simple Potential Functions for Simulating Liquid Water. *J. Chem. Phys.* **1983**, *79*, 926.

(28) Frisch, M. J.; Trucks, G. W.; Schlegel, H. B.; Scuseria, G. E.; Robb, M. A.; Cheeseman, J. R.; Montgomery, J. A., Jr.; Vreven, T.; Kudin, K. N.; Burant, J. C.; Millam, J. M.; Iyengar, S. S.; Tomasi, J.; Barone, V.; Mennucci, B.; Cossi, M.; Scalmani, G.; Rega, N.; Petersson, G. A.; Nakatsuji, H.; Hada, M.; Ehara, M.; Toyota, K.; Fukuda, R.; Hasegawa, J.; Ishida, M.; Nakajima, T.; Honda, Y.; Kitao, O.; Nakai, H.; Klene, M.; Li, X.; Knox, J. E.; Hratchian, H. P.; Cross, J. B.; Adamo, C.; Jaramillo, J.; Gomperts, R.; Stratmann, R. E.; Yazyev, O.; Austin, A. J.; Cammi, R.; Pomelli, C.; Ochterski, J. W.; Ayala, P. Y.; Morokuma, K.; Voth, G. A.; Salvador, P.; Dannenberg, J. J.; Zakrzewski, V. G.; Dapprich, S.; Daniels, A. D.; Strain, M. C.; Farkas, O.; Malick, D. K.; Rabuck, A. D.; Raghavachari, K.; Foresman, J. B.; Ortiz, J. V.; Cui, Q.; Baboul, A. G.; Clifford, S.; Cioslowski, J.; Stefanov, B. B.; Liu, G.; Liashenko, A.; Piskorz, P.; Komaromi, I.; Martin, R. L.; Fox, D. J.; Keith, T.; Al-Laham, M. A.; Peng, C. Y.; Nanayakkara, A.; Challacombe, M.; Gill, P. M. W.; Johnson, B.; Chen, W.; Wong, M. W.; Gonzalez, C.; Pople, J. A. *Gaussian 03; (Revision B.03) ed.*; Gaussian, Inc: Pittsburgh, PA, 2003.

(29) Schlegel, H. B. Optimization of Equilibrium Geometries and Transition Structures. *J. Comput. Chem.* **1982**, *3*, 214.

(30) Klauda, J. B.; Garrison, S. L.; Jiang, J.; Arora, G.; Sandler, S. I. HM-IE: Quantum Chemical Hybrid Methods for Calculating Interaction Energies. *J. Phys. Chem. A* **2004**, *108*, 107.

(31) Curtiss, L. A.; Redfern, P. C.; Raghavachari, K.; Rassolov, V.; Pople, J. A. Gaussian-3 theory using reduced Moller-Plesset order. *J. Chem. Phys.* **1999**, *110*, 4703.

(32) Curtiss, L. A.; Raghavachari, K.; Redfern, P. C.; Rassolov, V.; Pople, J. A. Gaussian-3 (G3) theory for molecules containing first and second-row atoms. *J. Chem. Phys.* **1998**, *109*, 7764.

(33) Dunning, T. H.; Peterson, K. A. Approximating the basis set dependence of coupled cluster calculations: Evaluation of perturbation theory approximations for stable molecules. *J. Chem. Phys.* **2000**, *113*, 7799.

(34) Brooks, B. R.; Bruccoleri, R. E.; Olafson, B. D.; States, D. J.; Swaminathan, S.; Karplus, M. CHARMM-a Program for Macromolecular Energy, Minimization, and Dynamics Calculations. *J. Comput. Chem.* **1983**, *4*, 187.

(35) Darden, T.; York, D.; Pedersen, L. Particle Mesh Ewald-an NLog(N) Method for Ewald Sums in Large Systems. *J. Chem. Phys.* **1993**, *98*, 10089.

(36) Wu, X. W.; Brooks, B. R. Isotropic periodic sum: A method for the calculation of long-range interactions. *J. Chem. Phys.* **2005**, *122*, 044107.

(37) Klauda, J. B.; Wu, X. W.; Pastor, R. W.; Brooks, B. R. Long-range Lennard-Jones and Electrostatic Interactions in Interfaces: Application of the Isotropic Periodic Sum Method. *J. Phys. Chem. B* **2007**, *111*, 4393.

(38) Ryckaert, J. P.; Ciccotti, G.; Berendsen, H. J. C. Numerical Integration of the Cartesian Equations of Motion of a System with Contraints: Molecular Dynamics of n-alkanes. *J. Comput. Phys.* **1977**, *23*, 327.

(39) Hoover, W. G. Canonical Dynamics-Equilibrium Phase-Space Distributions. *Phys. Rev. A* **1985**, *31*, 1695.

(40) Nosé, S.; Klein, M. L. A Study of Solid and Liquid Carbon Tetrafluoride Using the Constant Pressure Molecular-Dynamics Technique. *J. Chem. Phys.* **1983**, *78*, 6928.

(41) Andersen, H. C. Molecular-Dynamics Simulations at Constant Pressure and/or Temperature. *J. Chem. Phys.* **1980**, *72*, 2384.

(42) Allen, M. P.; Tildesley, D. J. *Computer Simulations of Liquids*; Clarendon Press: Oxford, 1987.

(43) Yeh, I. C.; Hummer, G. System-size dependence of diffusion coefficients and viscosities from molecular dynamics simulations with periodic boundary conditions. *J. Phys. Chem. B* **2004**, *108*, 15873.

(44) Borisenko, K. B.; Bock, C. W.; Hargittai, I. Intramolecular Hydrogen-Bonding And Molecular-Geometry Of 2-Nitrophenol From A Joint Gas-Phase Electron-Diffraction And Ab-Initio Molecular-Orbital Investigation. *J. Phys. Chem.* **1994**, *98*, 1442.

(45) Domenicano, A.; Schultz, G.; Hargittai, I.; Colapietro, M.; Portalone, G.; George, P.; Bock, C. W. Molecular Structure of Nitrobenzene in the Planar and Orthogonal Conformations. *Struct. Chem.* **1989**, *1*, 107.

(46) Shlyapochnikov, I. A.; Khrapkovskii, G. M.; Shamov, A. G. Structure and vibrational spectra of mononitroalkanes. *Russ. Chem. Bull.* **2002**, *51*, 940.

(47) Smith, G. D.; Jaffe, R. L. Quantum chemistry study of conformational energies and rotational energy barriers in n-alkanes. *J. Phys. Chem.* **1996**, *100*, 18718.

(48) Salam, A.; Deleuze, M. S. High-level theoretical study of the conformational equilibrium of n-pentane. *J. Chem. Phys.* **2002**, *116*, 1296.

(49) *Smithsonian Physical Tables*, 9th ed.; New York, 1954.

(50) Klauda, J. B.; Sandler, S. I. Ab Initio Intermolecular Potentials for Gas Hydrates and Their Predictions. *J. Phys. Chem. B* **2002**, *106*, 5722.

(51) Szabo, A.; Ostlund, N. S. *Modern Quantum Chemistry: Introduction to Advanced Electronic Structure Theory*; Dover Publication, Inc.: Mineola, NY, 1996.

(52) Toops, E. E. Physical Properties Of Eight High-Purity Nitroparaffins. *J. Phys. Chem.* **1956**, *60*, 304.

(53) Riddick, J.; Bunger, W.; Sakano, T. *Techniques of Chemistry: Organic Solvents, Physical Properties and Methods of Purification*, 4th ed.; Wiley: New York, 1986.

CT700191V